

Supporting Information

Metallic Contact between MoS₂ and Ni via Au Nanoglue

Xinying Shi, Sergei Posysaev, Marko Huttula, Vladimir Pankratov, Joanna Hoszowska, Jean-Claude Dousse, Faisal Zeeshan, Yuran Niu, Alexei Zakharov, Taohai Li, Olga Miroshnichenko, Meng Zhang, Xiao Wang, Zhongjia Huang, Sami Saukko, Diego López González, Sebastiaan van Dijken, Matti Alatalo, Wei Cao*

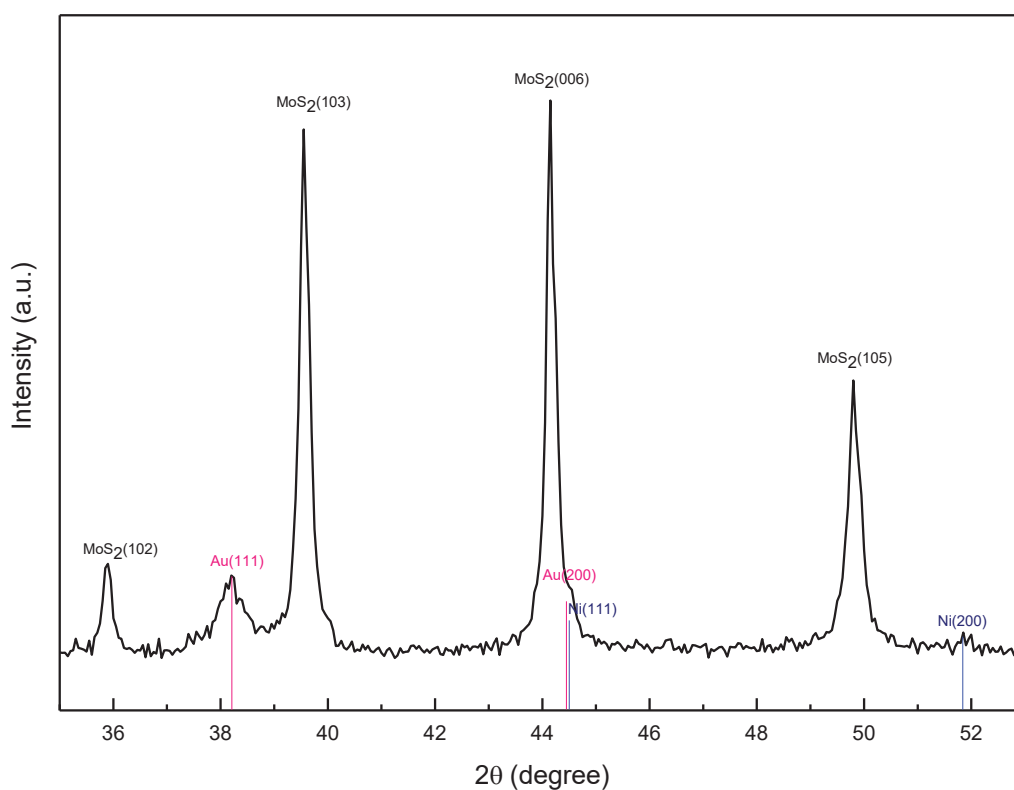


Figure S1. Powder X-ray diffraction of sample (MoS₂)_{92.9}Ni_{4.2}Au_{2.9}.

XRD patterns are indexed to phases of MoS₂ (102), (103), (006), (105), and Ni (111), (200). The Au (111) and (200) were also identified. A mean crystal size of AuNPs in the product was calculated to ~16 nm by fitting the Scherrer equation via the Rietveld method. It is worth

noting that, each Au particle shown in Figure 1c comprises of several Au crystals and Au particles in Figure 1g are only around 5 nm.

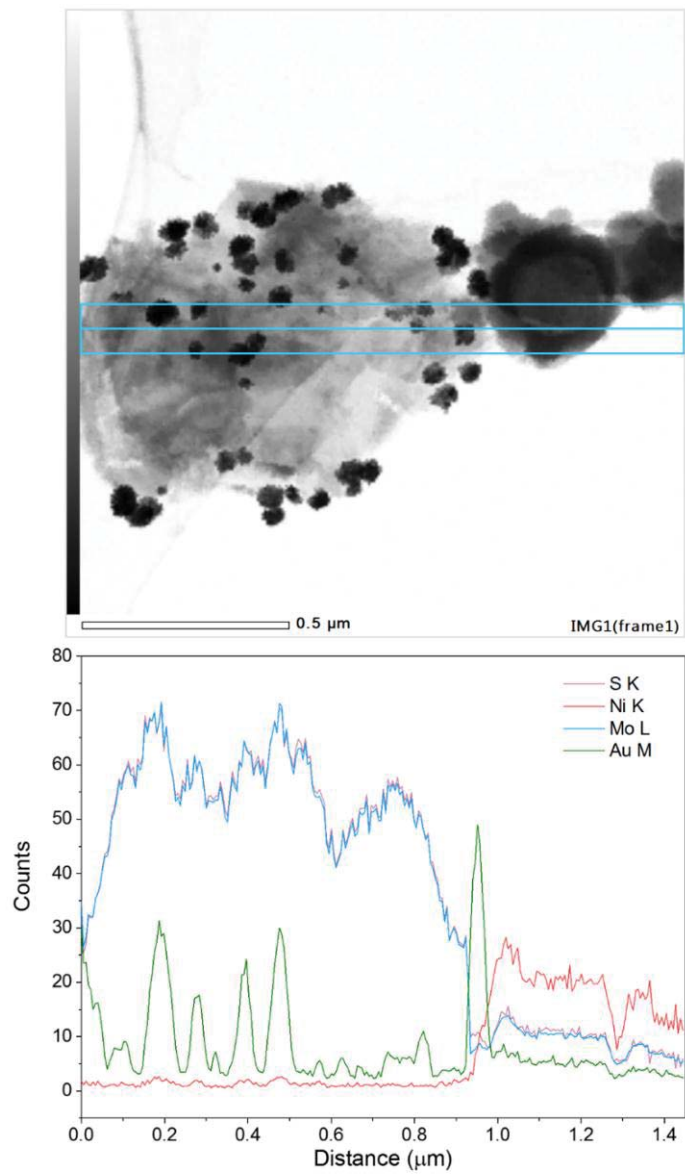


Figure S2. TEM-EDS line-scan results.

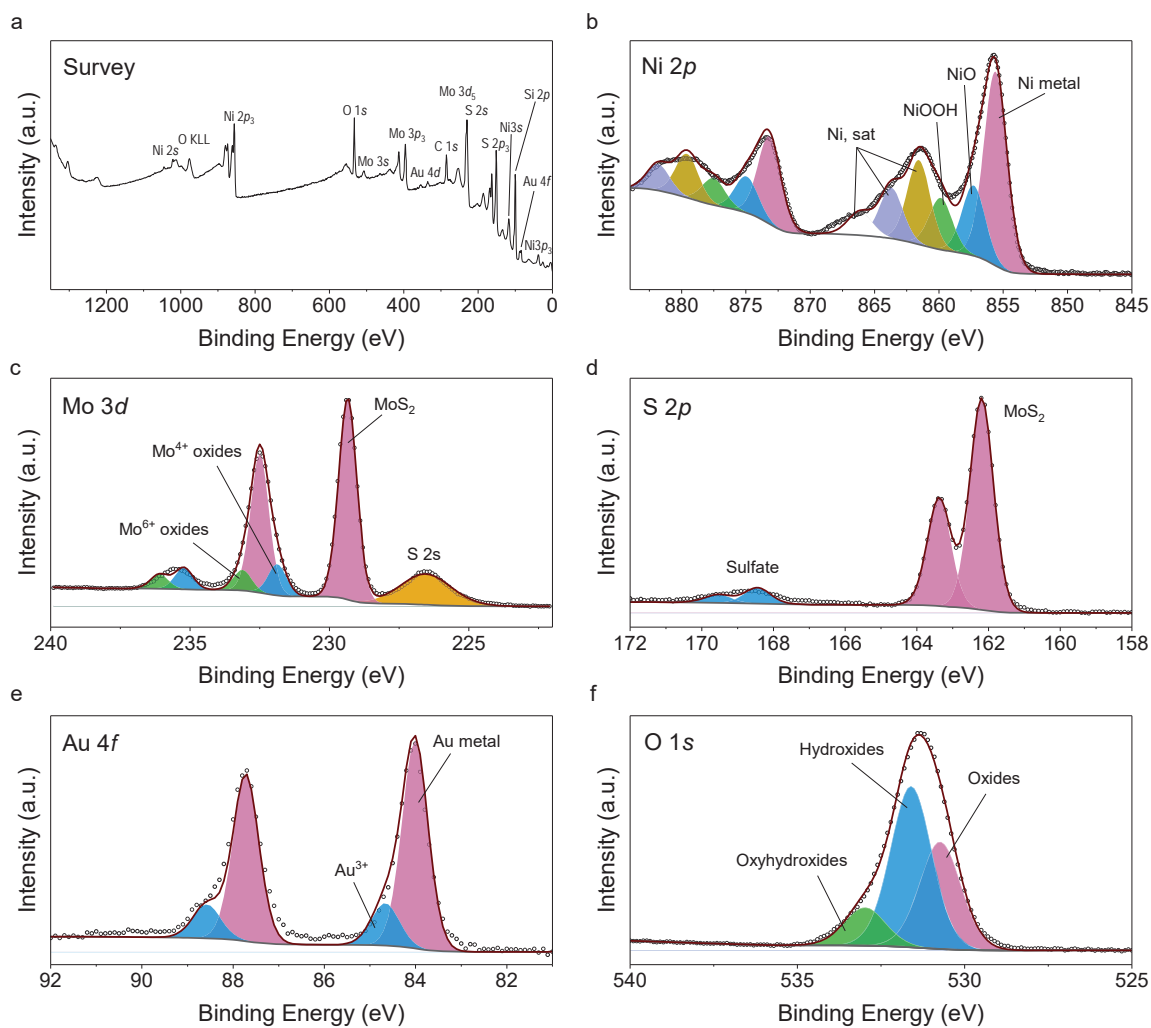


Figure S3. XPS analysis of the synthesized MoS₂-Au-Ni complex. (a) survey scan, (b) Ni 2p, (c) Mo 3d, (d) S 2s, (e) Au 4f, (f) O 1s. In panel b - e, experimental spectra (scatter plots) are deconvoluted into multi-peaks, and doublet peaks are shaded with identical colors. Plots in grey and wine colors are the baselines and fitting envelopes, respectively.

a		
Groups	Samples	Control samples
1	$(\text{MoS}_2)_{92.9}\text{Ni}_{4.2}\text{Au}_{2.9}$	$(\text{MoS}_2)_{93.6}\text{Ni}_{4.3}\text{Cl}_{2.1}$
2	$(\text{MoS}_2)_{94.2}\text{Ni}_{4.3}\text{Au}_{1.5}$	$(\text{MoS}_2)_{94.6}\text{Ni}_{4.4}\text{Cl}_1$
3	$(\text{MoS}_2)_{86.7}\text{Ni}_8\text{Au}_{5.3}$	$(\text{MoS}_2)_{88}\text{Ni}_{8.1}\text{Cl}_{3.9}$
4	$(\text{MoS}_2)_{89.1}\text{Ni}_{8.2}\text{Au}_{2.7}$	$(\text{MoS}_2)_{89.8}\text{Ni}_{8.2}\text{Cl}_2$

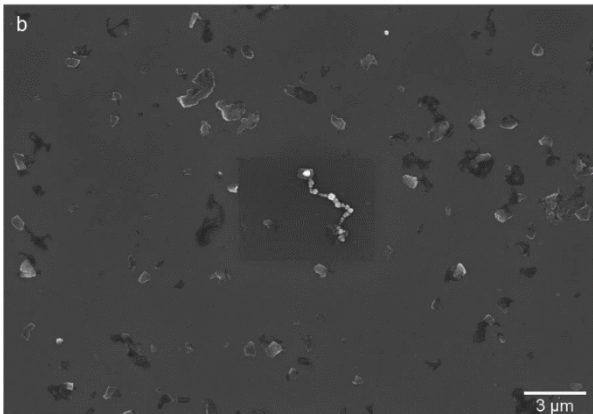


Figure S4. Synthesis and characterization of samples in control group. (a) List of synthesized samples and comparative ones in control group. The molar ratios of MoS_2 , Ni and Cl were kept the same in each group, and converted to weight percentages listed in the table. (b) SEM image of sample $(\text{MoS}_2)_{93.6}\text{Ni}_{4.3}\text{Cl}_{2.1}$, which was designed to make comparison with sample $(\text{MoS}_2)_{92.9}\text{Ni}_{4.2}\text{Au}_{2.9}$. In the figure, most MoS_2 flakes are in multilayer form, and well separated from NiNPs. Even in the case that NiNPs appeared in the surrounding of MoS_2 , NiNPs are more likely to aggregate together rather than joining to the MoS_2 flakes.

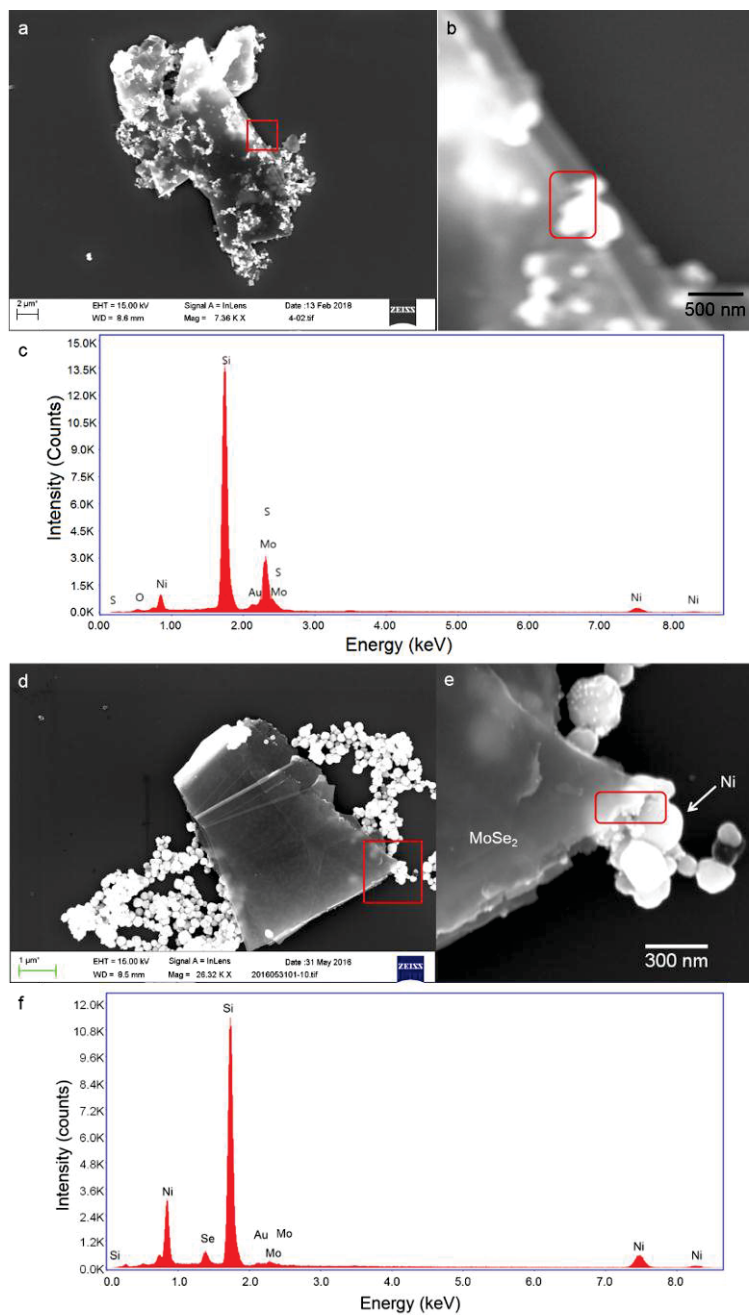


Figure S5. Introduce NiNPs onto large-scale MoS₂ and MoSe₂ crystals. (a) NiNPs decorated on MoS₂ crystals. (b) A zoomed-in region marked in (a). (c) EDS spectrum of the interface region marked in (b). (d) NiNPs decorated on MoSe₂ crystals. (e) A zoomed-in region shown in (d). (f) EDS spectrum of the interface region shown in (e). A strong peak at 1.7 keV comes from the Si substrate.

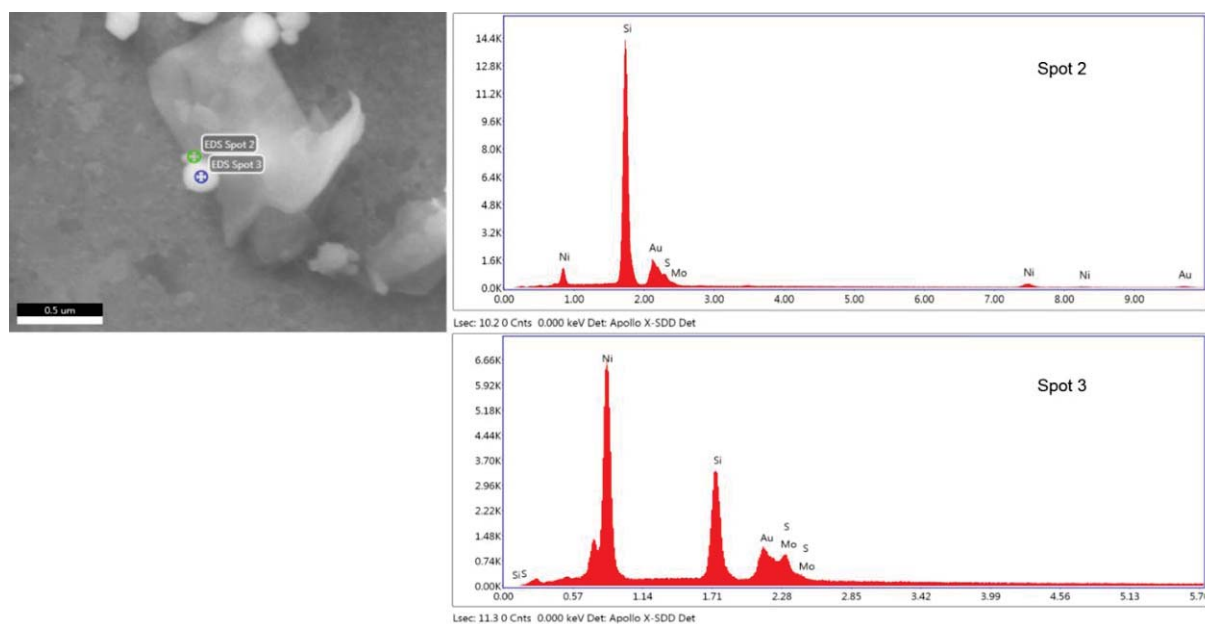


Figure S6. EDS determination. Before conductive-AFM measurements, samples were first investigated under SEM for efficient locating on candidate flakes. Then EDS was employed for elemental confirmation. Silicon signals come from the Si substrates.

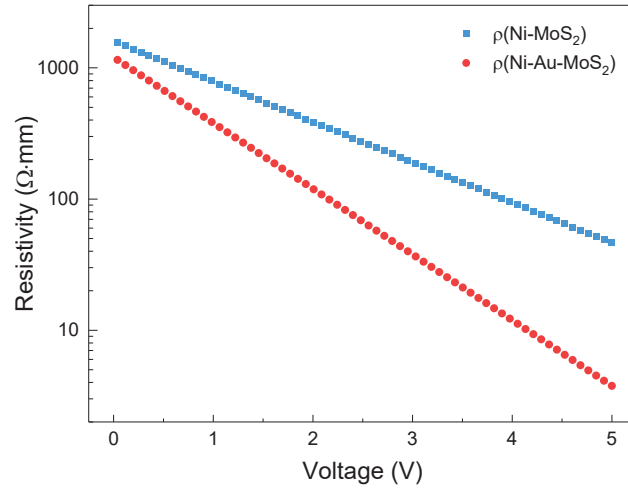


Figure S7. Estimation of electrical resistivity of Ni-Au-MoS₂ and Ni-MoS₂ contacts.

The electrical resistivity of the two contacts are calculated by Equation S1:

$$\rho = R_c \cdot A / L \quad (1)$$

where ρ , R_c , A , and L represent electrical resistivity, contact resistance, contact area and contact length, respectively. For a rough estimation, R_c is approximately replaced by R_{t1} and R_{t2} . Taking the tip area as the contact area and the distance between tip and Au substrate film as the contact length, the electrical resistivity can be then calculated.

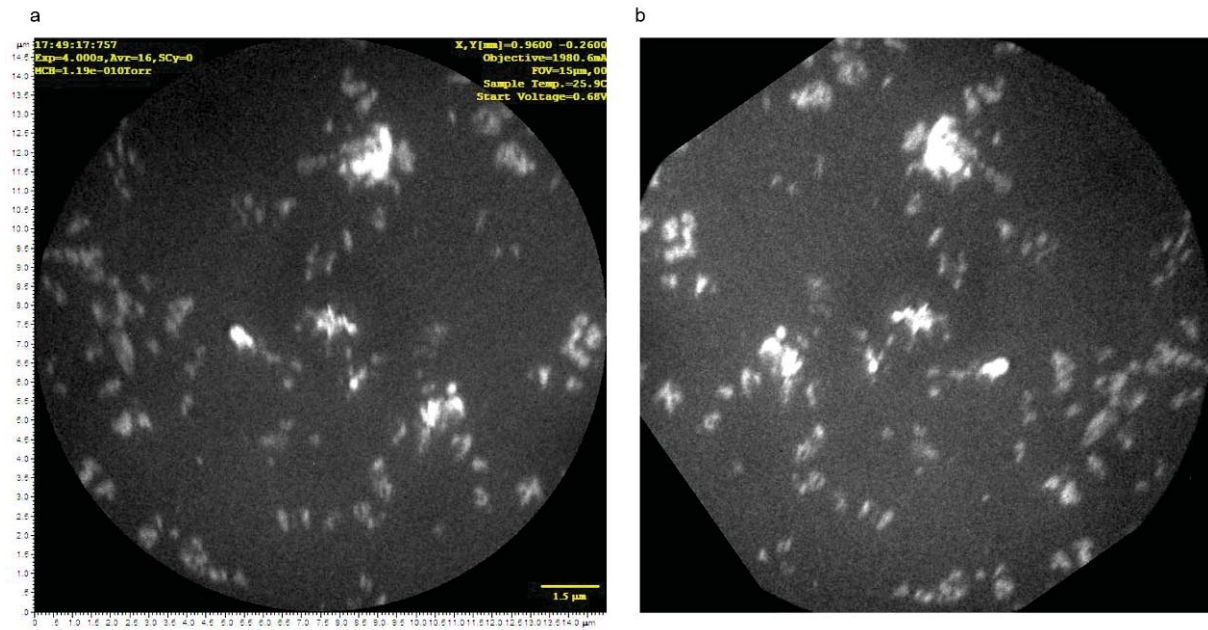


Figure S8. Full view of (a) original and (b) rotated PEEM images.

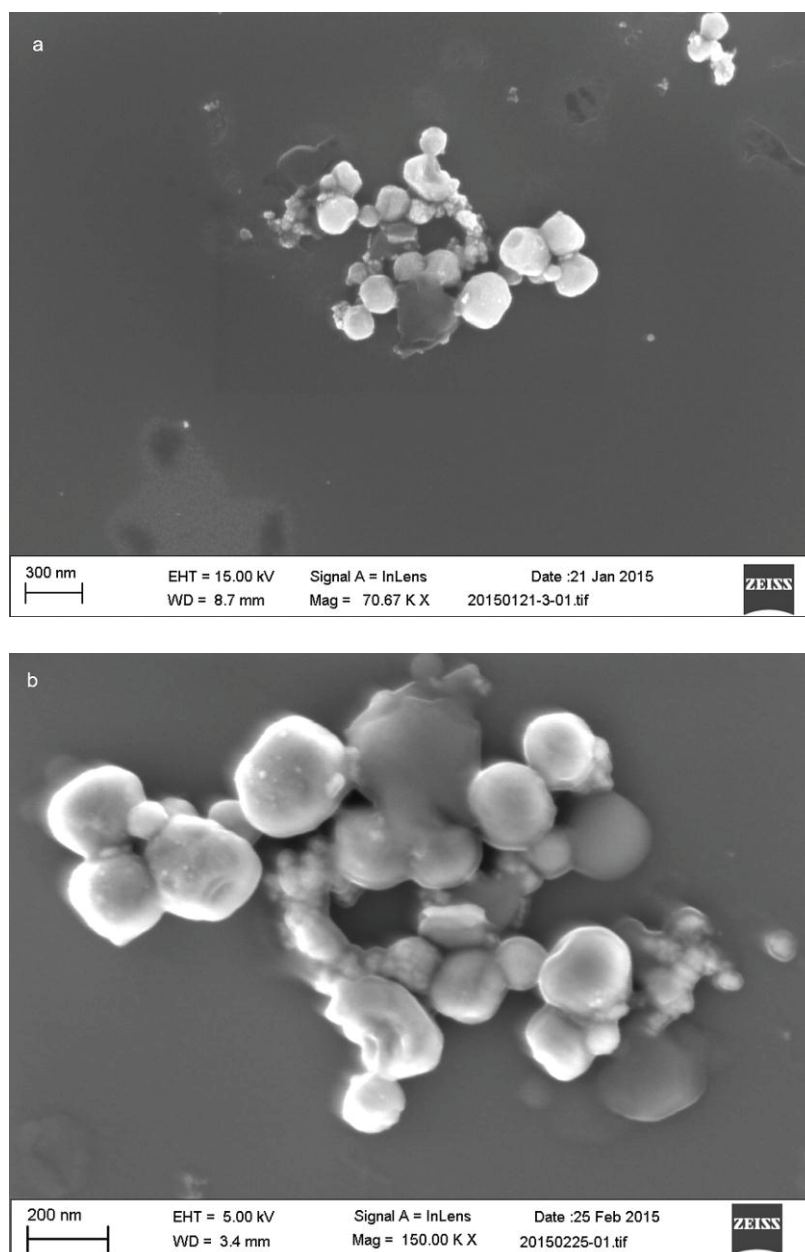


Figure S9. SEM image taken before and after synchrotron radiation based PEEM experiments. (a) Before PEEM, taken on 21 Jan. 2015. (b) After PEEM, taken on 25 Feb. 2015. Both images were taken at the Center of Microscopy and Nanotechnology, Oulu, Finland. PEEM experiments were carried out on 15 Feb. 2015, at Max IV laboratory, Lund, Sweden. The joint regions between MoS₂ and Ni are kept stable and intact after the exposure to synchrotron radiation and electron beam radiation.

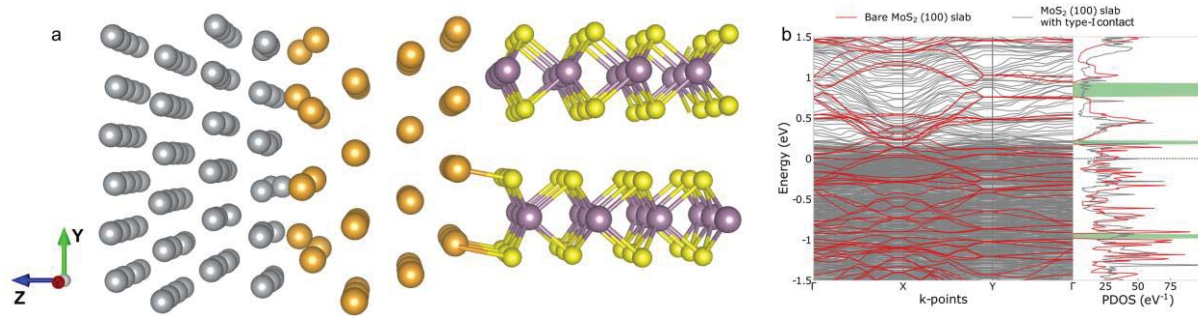


Figure S10. (a) Optimized geometry of the $\text{Mo}_{24}\text{S}_{48}\text{Au}_{46}\text{Ni}_{92}$ supercell. (b) Band structure of the MoS_2 (100) surface without contact is plotted with red curves, while gray curves represent band structure of $\text{Mo}_{24}\text{S}_{48}\text{Au}_{46}\text{Ni}_{92}$ supercell. The silver, orange, purple and yellow spheres represent the Ni, Au, Mo and S atoms, respectively.

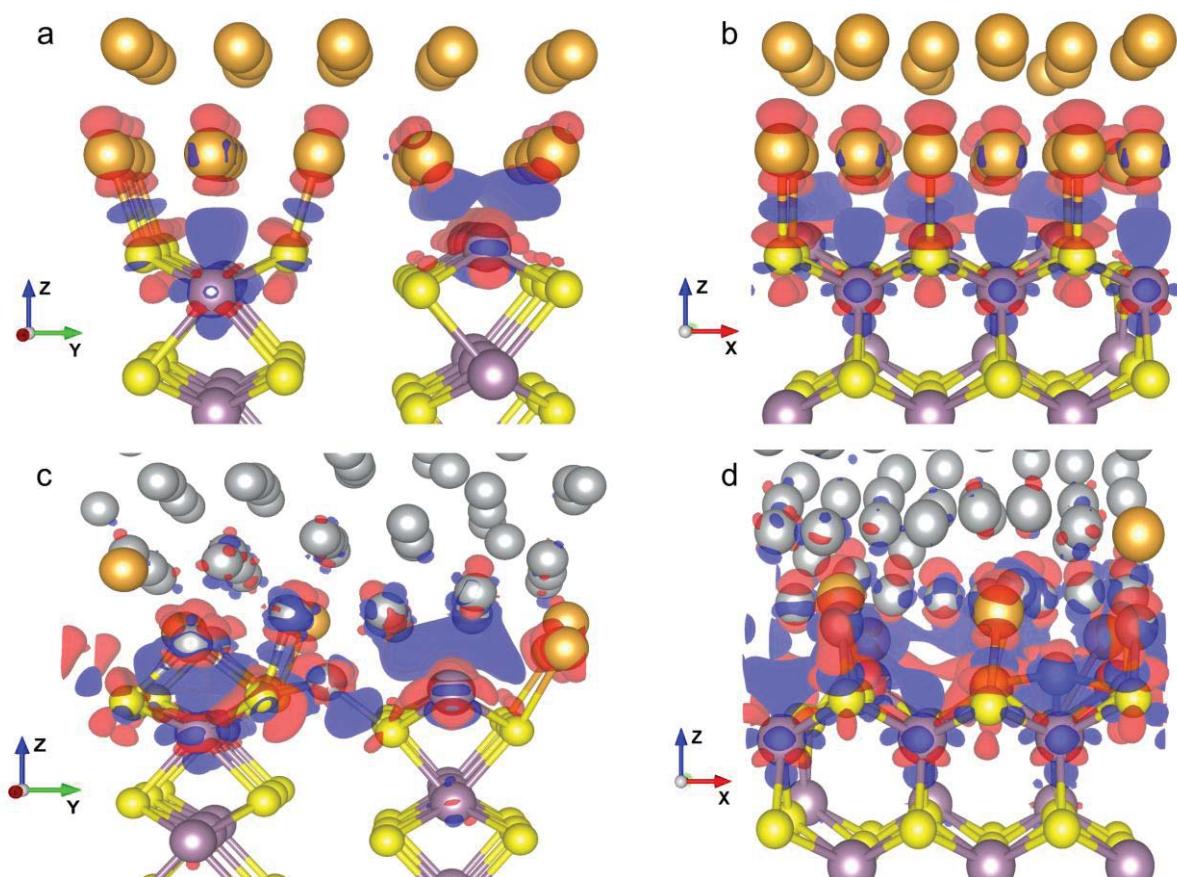


Figure S11. Geometric structures and charge density difference for both models. The red region shows the charge accumulation, while the blue region represents the charge depletion. Panel (a) and (b) present optimized geometry of the $\text{Mo}_{24}\text{S}_{48}\text{Au}_{30}$ supercell (type-I contact). Panel (c) and (d) are optimized geometry of the $\text{Mo}_{24}\text{S}_{48}\text{Au}_6\text{Ni}_{72}$ supercell (type-II contact). The isosurface value is $0.005 e/\text{\AA}^3$.

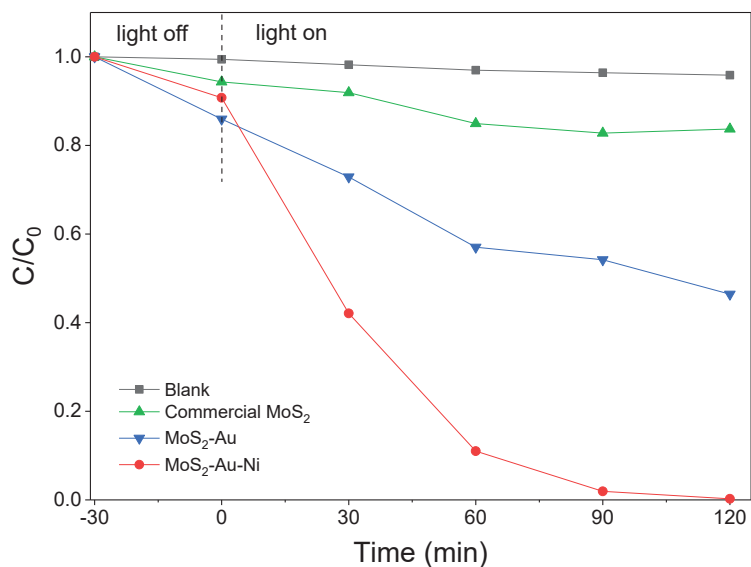


Figure S12. Photodegradation of methylene blue (MB) under UV light irradiation. During photolysis process (without catalyst, see the *blank* curve), the concentration of MB is kept nearly unchanged, suggesting that the self-degradation is slow even when exposed under UV irradiation. Commercial MoS₂ and Au-decorated MoS₂ show weak photocatalytic ability. In the case of synthesized MoS₂-Au-Ni ternary complex, the concentration of MB reduces drastically during the first 30 min, and is almost degraded after 90 min.

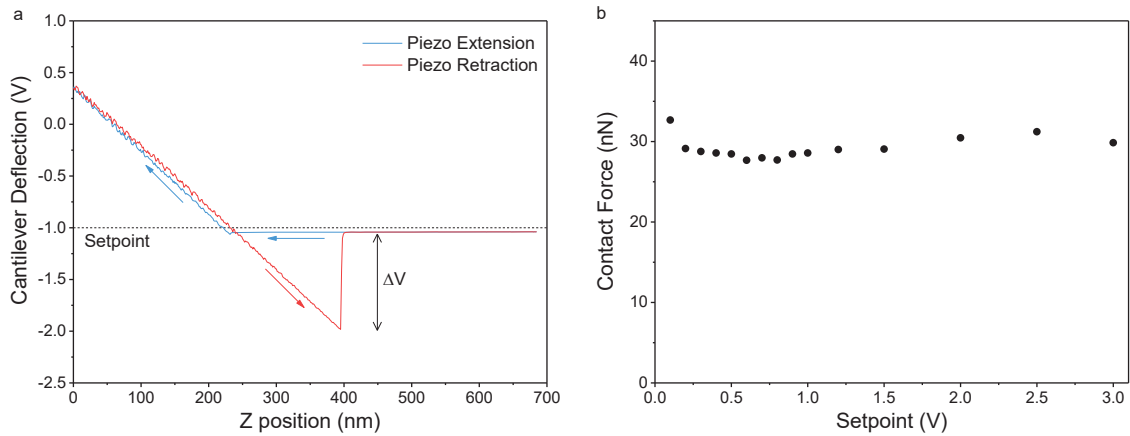


Figure S13. Investigation of the reliability of C-AFM measurements. (a) Cantilever performance under the setpoint of 1.0 V. (b) Contact force under different setpoint voltages.

The contact force can be calculated by Hooke's Law: $F = k \cdot d$, where k is the spring constant of the cantilever (0.18 N/m for the tip used in this work) and d is deflection. The deflection can be obtained by the relation: $d = \Delta V \cdot S$, where ΔV is the difference between the minimum cantilever deflection and the deflection in the original state, S is deflection sensitivity which can be calculated by the slope of Piezo Retraction curve.

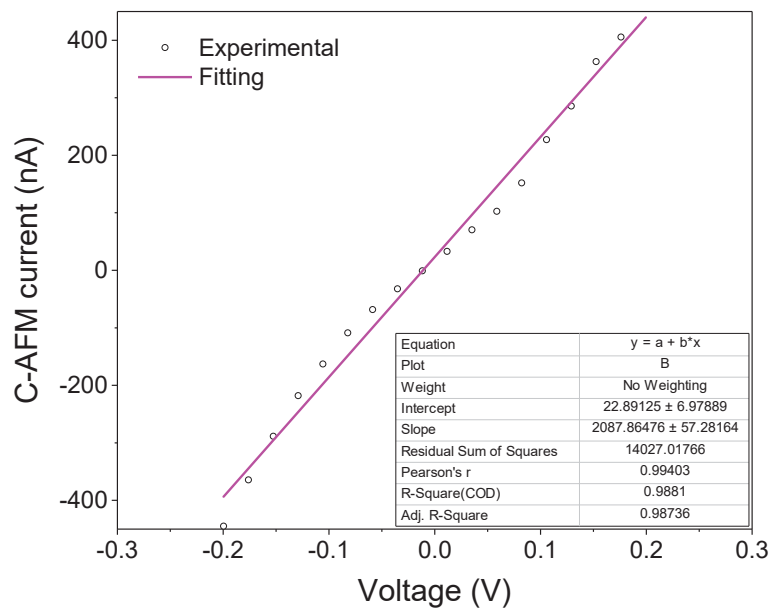


Figure S14. I - V curve recorded when AFM tip probed directly on Au substrate film.